Robustness analysis of Passivity-based Controllers for Complementarity Lagrangian Systems

Jean-Matthieu Bourgeot, Bernard Brogliato

INRIA

Robustness analysis of Passivity-based Controllers for Complementarity Lagrangian Systems

Jean-Matthieu Bourgeot — Bernard Brogliato

N° 5385

Novembre 2004

THÈME 4

R apport de recherche

Robustness analysis of Passivity-based Controllers for Complementarity Lagrangian Systems

Jean-Matthieu Bourgeot , Bernard Brogliato

Thème 4 — Simulation et optimisation
de systèmes complexes
Projets Bipop

Abstract: In this paper we study the robustness of tracking controllers for Lagrangian systems subject to frictionless unilateral constraints. The stability analysis incorporates the hybrid and nonsmooth dynamical features of the overall system. This work provides details on the robustness of such controllers with respect to the modelling errors of the dynamic, the uncertainty on the constraint position, and with respect to the measurement noise.

Key-words: Unilateral Constraint, Nonsmooth Mechanics, Hybrid System, Lyapunov Stability

Analyse de robustesse de contrôleurs basés sur la passivité pour des systèmes lagrangiens de complèmentarité

Résumé : Dans ce papier nous faisons une étude de robustesse pour un contrôleur de poursuite de trajectoires pour des systèmes Lagrangiens soumis à des contraintes unilatérales sans frottements. L'analyse de stabilité tient compte des aspects hybrides et non réguliers du système bouclé. Ce travail fournit des détails sur la robustesse de tels contrôleurs vis-à-vis des incertitudes sur les paramètres du modèle dynamique, vis-à-vis d'une mauvaise connaissance de la position de la contrainte, et enfin vis-à-vis du bruit de mesure.

Mots-clés : Contrainte Unilatérale, Mécanique Non-Régulière, Système Hybride, Stabilité de Lyapunov

1 Introduction

The focus of this paper is the tracking control of a class of nonsmooth fully actuated Lagrangian systems subject to frictionless unilateral constraints on the position. Such systems may *a priori* evolve in three different phases of motion:

i) A free motion phase,

ii) A permanently constrained phase with a non-zero contact force,

iii) A transition phase whose goal is to stabilize the system on some constraint surface.

The controller used in this paper was fully detailed in [1]. The present paper gives numerical results on the robustness of two passivity based controllers.

1.1 Dynamics

Let $X \in \mathbb{R}^n$ denote the vector of generalized coordinates. The systems we study in this paper are complementarity Lagrangian systems. The dynamics is:

$$\begin{cases} M(X)\ddot{X} + C(X,\dot{X})\dot{X} + G(X) = u + \nabla F(X)\lambda_X \\ F(X) \geq 0, \quad F(X)^T \lambda_X = 0, \quad \lambda_X \geq 0 \\ \text{Collision rule} \end{cases} \quad (1)$$

where $M(X)$ is the positive definite inertia matrix, $F(X) \in \mathbb{R}^m$ represents the distance to the constraints, $\lambda_X \in \mathbb{R}^m$ are the Lagrangian multipliers associated to the constraints, $u \in \mathbb{R}^n$ is the vector of generalized torque inputs, $C(X,\dot{X})$ is the matrix of Coriolis and centripetal forces, $G(X)$ contains conservative forces. ∇ denotes the Euclidean gradient.

The impact times will be denoted generically as t_k in the following. The admissible domain Φ is a closed domain in the configuration space where the system can evolve, i.e. $\Phi = \{X | F(X) \geq 0\}$. The boundary of Φ is denoted as $\partial\Phi$. A collision rule is needed to integrate the system in (1) and to render the set Φ invariant. In this work, it is chosen as in [6]:

$$\dot{X}(t_k^+) = -e_n \dot{X}(t_k^-) + (1 + e_n) \underset{z \in T_\Phi(X(t_k))}{\arg\min} \frac{1}{2}[z - \dot{X}(t_k^-)]^T M(X(t_k))[z - \dot{X}(t_k^-)] \quad (2)$$

where $\dot{X}(t_k^+)$ is the post impact velocity, $\dot{X}(t_k^-)$ is the pre-impact velocity, $T_\Phi(X(t))$ the tangent cone to the set Φ at $X(t)$ and e_n is the restitution coefficient, $e_n \in [0,1[$.

1.2 Cyclic task

In this paper we restrict ourselves to a specific task, or trajectory: a succession of free and constrained phases $\Omega_{k_{cyc}}$. During the transition between a free and a constrained phase,
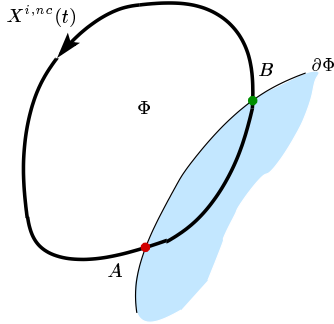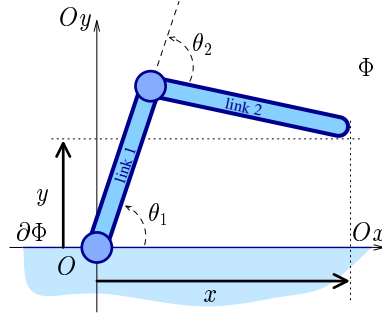
Figure 1: Unconstrained trajectory

Figure 2: Planar 2dof robotic arm

the dynamic system passes into a transition phase $I_{k_{cyc}}$. In the time domain one gets a representation as :

$$\mathbb{R}^+ = \Omega_0 \cup I_0 \cup \Omega_1 \cup \Omega_2 \cup I_1 \cup ... \cup \Omega_{2k_{cyc}-1} \cup \Omega_{2k_{cyc}} \cup I_{k_{cyc}} \cup ... \qquad (3)$$

where $\Omega_{2k_{cyc}}$ denotes the time intervals associated to free-motion phases and $\Omega_{2k_{cyc}+1}$ those for constrained-motion phases. The order of the phases is important but the initial phase may be Ω_0 or I_0 or Ω_1. Transition between constrained-motion and free motion does not spawn to a specific phase because there is no discontinuity of the state vector.

As explained in [1] the control strategy and stability analysis have to cope with the fact that the time of the first impact, and the time of detachment are unknown. Then four different trajectories are used in the analysis: On the first hand, the signal $X_d^\star(\cdot)$ in the control input (Fig. 3(a)). This trajectory imposes impacts when the tracking error is not zero (imposing impacts improves the robustness if the constraint position knowledge is bad). The trajectory $X_d^\star(\cdot)$ tends to the tangential approach (noted $X^{i,nc}(\cdot)$ on Fig. 3(b)) when $k_{cyc} \to \infty$. On the other hand, the signal $X_d(\cdot)$ enters the Lyapunov function (Fig. 3(c)); this trajectory differs from $X_d^\star(\cdot)$ because between B and C the point $(q_d^\star, \dot{q}_d^\star)$ is not reachable, then $X_d(\cdot)$ is set on the surface $\partial\Phi$ after the first impact of each cycle. The trajectory $X_d(\cdot)$ tends to $X^{i,c}(\cdot)$ (see Fig. 3(d)) which is the impactless trajectory of the system when tracking is perfect.

> *This is the major discrepancy compared to unconstrained motion control in which all four trajectories are the same, usually denoted as $X_d(\cdot)$.*

We see here the hybrid aspect of the convergence analysis. On one hand, we need to guarantee the continuous convergence $(X(\cdot) \to X_d(\cdot))$, and on the other hand the discrete convergence $(X_d(\cdot) \to X^{i,c}(\cdot))$ over the cycles k_{cyc}. From the user point of view, the tracking error is $X(\cdot) - X^{i,c}(\cdot)$ (see sec. 4 for illustration on a particular example).

The cycles $\Omega_{2k_{cyc}} \cup I_{k_{cyc}} \cup \Omega_{2k_{cyc}+1}$ duration is not arbitrary set since it depends on phases $I_{k_{cyc}}$ duration, which in turn may depend on control and physical parameters (see an illustration in sec. 4).
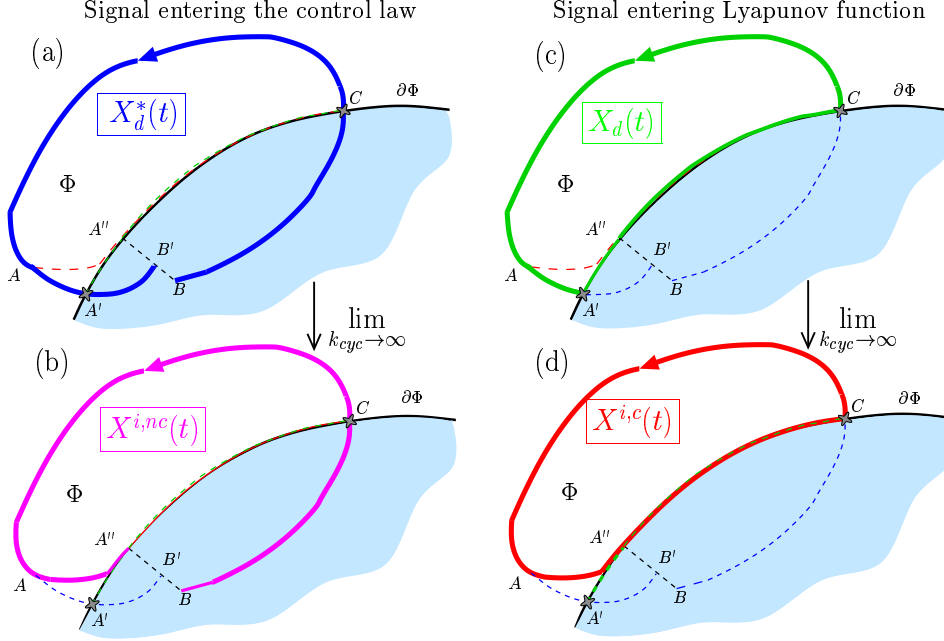
Signal entering the control law   Signal entering Lyapunov function

Figure 3: The closed-loop desired trajectories

2 Stability framework

The stability criterion used in this paper is an extension of the Lyapunov second method adapted to closed loop mechanical system with unilateral constraints and has been proposed in [1] [2] and [3]. Let $x(\cdot)$ denote the state of the closed-loop system in (1) with some feedback controller $u(X, \dot{X}, t)$.

Definition 1 (Ω-weakly stable system) *The closed-loop system is Ω-weakly stable if for each $\epsilon > 0$, there exists $\delta(\epsilon) > 0$ such that $\parallel x(0) \parallel \leq \delta(\epsilon) \Rightarrow \parallel x(t) \parallel \leq \epsilon$ for all $t \geq 0$, $t \in \Omega = \cup_{k_{cyc} \geq 0} \Omega_{k_{cyc}}$. Asymptotic weak stability holds if in addition $x(t) \longrightarrow 0$ as $t \longrightarrow +\infty$, $t \in \Omega$. Practical weak stability holds if there is a ball centered at $x = 0$, with radius $R > 0$, and such that $x(t) \in B(0, R)$ for all $t \geq T$; $T < +\infty$, $t \in \Omega$, $R < +\infty$.* ∎

Let us define $P_{\Sigma_{\mathcal{I}}}$, the closed-loop impact Poincaré map that corresponds to the section $\Sigma_{\mathcal{I}}^- = \{x | F_i(X) = 0, \dot{X}^T \nabla F_i(X) < 0, i \in \mathcal{I}\}$, which is a hypersurface of codimension $\alpha =$

card($\mathcal{I}$). Let us introduce the positive definite function $V(\cdot)$ that will serve in the subsequent analysis. Let $V_{\Sigma_\mathcal{I}}$ denote the restriction of V to $\Sigma_\mathcal{I}$.

Definition 2 (Strongly stable system) *The system is said strongly stable if: (i) it is Ω-weakly stable, (ii) on phases $I_{k_{cyc}}$, $P_{\Sigma_\mathcal{I}}$ is Lyapunov stable with Lyapunov function $V_{\Sigma_\mathcal{I}}$, and (iii) the sequence $\{t_k\}_{k\in\mathbb{N}}$ has a finite accumulation point $t_\infty < +\infty$.* ■

In [1], two claims are presented which are useful to prove the stability of Lagrangian systems with respect to the definitions 1 and 2.

3   Tracking controller framework

In this section we briefly develop the tracking controller strategy used in this paper. A more elaborate description is available in [1] with a complete stability analysis. In this paper we focus on the simulations and robustness aspects.

3.1   Controller Structure

To make the controller design easier the dynamical equations (1) are considered in the generalized coordinates introduced in [5]. After transformation in the new coordinates $q = [q_1, q_2]^T$, $q_1 = [q_1^1 \ldots q_1^m]^T$, $q = Q(X) \in \mathbb{R}^n$, the dynamical system is as follows :

$$\begin{cases} M_{11}(q)\ddot{q}_1 + M_{12}(q)\ddot{q}_2 + C_1(q,\dot{q})\dot{q} + g_1(q) = T_1(q)U + \lambda \\ M_{21}(q)\ddot{q}_1 + M_{22}(q)\ddot{q}_2 + C_2(q,\dot{q})\dot{q} + g_2(q) = T_2(q)U \\ q_1^i \geq 0, \quad q_1^i \lambda_i = 0, \quad \lambda_i \geq 0, \ 1 \leq i \leq m \\ \text{Collision rule} \end{cases} \tag{4}$$

The vector q_1 denotes the constraint coordinate and q_2 denotes the free coordinate. The controller developed in this paper uses three different low-level control laws for each phase $\Omega_{2k_{cyc}}$, $\Omega_{2k_{cyc}+1}$ and $I_{k_{cyc}}$:

$$T(q)U = \begin{cases} U_{nc} & = U_{nc}(q, q_d^\star, \dot{q}, \dot{q}_d^\star, \ddot{q}, \ddot{q}_d^\star) \\ U_t & = U_{nc}(q, q_d^\star, \dot{q}, \dot{q}_d^\star, \ddot{q}, \ddot{q}_d^\star) \quad \text{before the first impact} \\ U_t & = U_{nc}(q, q_d^\star, \dot{q}, 0, \ddot{q}, 0) \quad \text{after the first impact} \\ U_c & = U_{nc} - P_d + K_f(P_q - P_d) \end{cases} \tag{5}$$

where $-P_d + K_f(P_q - P_d)$ is the force/position feedback which is added during the $\Omega_{2k_{cyc}+1}$ phases. A supervisor switches between these three control laws. The overall structure of the control strategy is shown on Fig. 4. The transition control law corresponds to the non-constraint one with $q_d^\star(t)$ frozen ($q_d^\star = \dot{q}_d^\star = 0$), and the constraint law correspond to the sum of non-constraint control and a control in force. The asymptotic stability of this scheme makes the system land on the constraint surfaces tangentially after enough cycles

of constraints/free motions (one cycle $= \Omega_{2k_{cyc}} \cup I_{k_{cyc}} \cup \Omega_{2k_{cyc}+1}$). Asymptotically the transitions between free motion phases and permanently constraint phases are done without any collision.
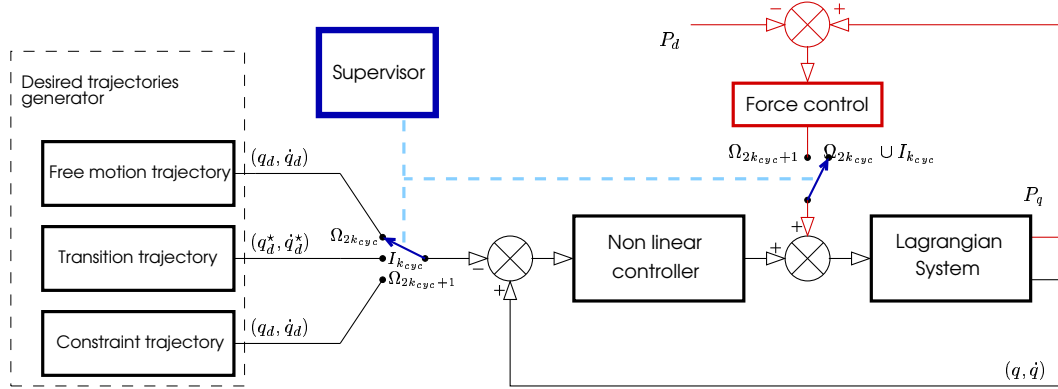

Figure 4: Structure of the controller

As observed in the introduction, a control strategy which consists of attaining the surface $\partial \Phi$ tangentially and without incorporating impacts in the stability analysis, cannot work in practice due to its lack of robustness. In view of this, the control law for the transition phase is defined in order :

- To make the system hit the constraint surface (and then dissipate energy during impacts) if the tracking error is not zero.

- To make the system approach the constraint surface tangentially (without rebound) if the tracking is perfect.

These two situations are conflicting. On the other hand the coupling between q_1 and q_2 in (4), makes the asymptotic stability quite difficult to obtain if velocities are subject to discontinuities: any velocity jump at t_k implies $\sigma_V(t_k) > 0$ when $V \equiv 0$. Hence if the transition phase is constructed with impacts, one has to find a manner to get $V(t_f^{k_{cyc}}) = 0$ in order to force the system to remain on the desired trajectory $X_d(\cdot)$ (here $q_d(\cdot)$). This is not obvious in general and defining $q_d^{\star}(\cdot)$ as done below is a way to get the result.

3.2 Design of the desired trajectory

During the transition phase the control signal $q_d^{\star}(t)$ is defined as follows (see Fig. 5 for $q_{1d}^{\star}(\cdot)$, where A, A', B', B and C correspond to Fig. 3). Let us define:

- $\tau_0^{k_{cyc}}$ is chosen by the designer as the start of the transition phase,
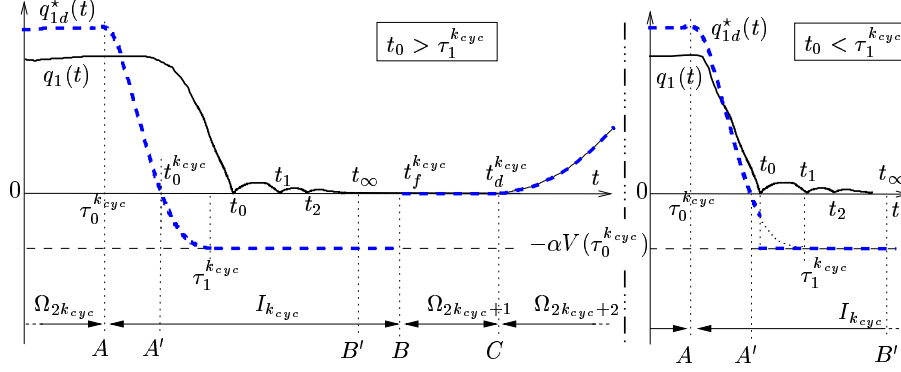
Figure 5: Trajectory $q_{1d}^{\star}(t)$

- $t_0^{k_{cyc}}$ is the time corresponding to $q_{1d}^{\star}(t_0^{k_{cyc}})=0$,
- t_0 corresponds to the first impact,
- t_{∞} corresponds to the finite accumulation point of the sequence $\{t_k\}_{k \geq 0}$,
- $t_f^{k_{cyc}}$ is the end of the transition phase,
- $\tau_1^{k_{cyc}}$ is such that $q_{1d}^{\star}(\tau_1^{k_{cyc}}) = -\alpha V(\tau_0^{k_{cyc}})$ and $\dot{q}_{1d}^{\star}(\tau_1^{k_{cyc}}) = 0$.
- $\Omega_{2k_{cyc}+1} = [t_f^{k_{cyc}}, t_d^{k_{cyc}}]$.

On $[\tau_0^{k_{cyc}}, t_0)$, we impose that $q_d^{\star}(t)$ is twice differentiable, and $q_{1d}(t)$ decreases towards $-\alpha V(\tau_0^{k_{cyc}})$ on $[\tau_0^{k_{cyc}}, \tau_1^{k_{cyc}}]$. In order to cope with the coupling between q_1 and q_2 ($M_{12} \neq 0$), the signal $q_{2d}^{\star}(t) \in C^2(\mathbb{R}^+)$ is frozen during the transition phase, i.e.: $q_{2d}^{\star}(t) = q_{2d}^{\star}$, $\dot{q}_{2d}^{\star}(t) = 0$ on $[\tau_0^{k_{cyc}}, t_{\infty}]$.

On $(t_0, t_f]$, we define q_d and $q_d^{\star}$ as: $q_d = (0, q_{2d}^{\star})^T$, $q_d^{\star} = (-\alpha V(\tau_0^{k_{cyc}}), q_{2d}^{\star})^T$.

On $[t_f^{k_{cyc}}, t_d^{k_{cyc}}]$ we set $q_d = [0, q_{2d}(t)]^T$. The purpose of $q_d^{\star}$ is to create a "virtual" potential force which stabilizes the system on $\partial\Phi$ even if the position of the constraint is uncertain. Consequently the fixed point $(q_d, \dot{q}_d)$ of the complementarity system is used in the expression of the Lyapunov function ($\tilde{q} = q - q_d$), whereas the unreachable fixed point $q_d^{\star}$ is used in the control law. In summary, after the first impact at t_0, $q_{1d}(\cdot)$ is set to zero while in case $\tau_1^{k_{cyc}} > t_0$, $q_{1d}^{\star}(\cdot)$ is set to $-\alpha V(\tau_0^{k_{cyc}})$ (in other words U_t switches as indicated in (5)) . Since $\dot{q}_{1d}(t_0^-) \neq 0$ and $q_{1d}(t_0^-) \neq 0$ in general, the trajectory $q_{1d}(\cdot)$ behaves like in a sort of plastic collision ($e_n = 0$). With respect to Fig. 3, one has $\tau_0^{k_{cyc}}$ at A, t_{∞} at B', t_0 at A', $t_d^{k_{cyc}}$ at C, and B at $t_f^{k_{cyc}}$ (the term $-P_d - K_f P_d$ defines the signal $X_d^{\star}(\cdot)$ between B and C on Fig. 3). If $V(\tau_0^{k_{cyc}}) = 0$ then A'' corresponds to the time $\tau_1^{k_{cyc}}$.

The piece of curve AA' on Fig. 3 is normal to $\partial\Phi$. The closed-loop desired trajectory $X^{i,c}(\cdot)$ is defined as $q^{i,c}(t) = q_d^\star(t)$ on $\Omega_{2k_{cyc}}$, $q^{i,c}(t) = q_d^\star(t)$ with $\alpha = 0$ on $I_{k_{cyc}}$, and $q_1^{i,c}(t) = 0$ on $\Omega_{2k_{cyc}+1}$, $q_2^{i,c}(t) = q_{2d}^\star(t)$ on $\mathbb{R}^+$. It is impactless.

The choice for $q_d^\star(.)$ is done to get $\sigma_V(t_k) \le 0$ on $I_{k_{cyc}}$

3.3 Two control laws for the nonlinear controller block (on Fig. 4)

3.3.1 Hybrid Paden-Panja scheme.

The control law used in this first scheme is based on the controller presented in [7], originally designed for free-motion position and velocity global asymptotic tracking. Let us propose:

$$U_{nc} = M(q)\ddot{q}_d^\star + C(q,\dot{q})\dot{q}_d^\star + g(q) - \gamma_1(q - q_d^\star) - \gamma_2(\dot{q} - \dot{q}_d^\star) \tag{6}$$

where $\gamma_1 > 0$, $\gamma_2 > 0$. The Lyapunov function associated to this control law is:

$$V(t,\tilde{q},\dot{\tilde{q}}) = \frac{1}{2}\dot{\tilde{q}}^T M(q)\dot{\tilde{q}} + \frac{1}{2}\gamma_1 \tilde{q}^T \tilde{q}, \text{ with } \tilde{q}(\cdot) = q(\cdot) - q_d(\cdot) \tag{7}$$

3.3.2 Hybrid Slotine-Li scheme.

For the second scheme, the nonlinear controller block (on Fig. 4) is based on the scheme presented in [8]. Let us propose the following:

$$U_{nc} = M(q)\ddot{q}_r + C(q,\dot{q})\dot{q}_r + g(q) - \gamma_1 s \tag{8}$$

where $s = \dot{\tilde{q}} + \gamma_2 \tilde{q}$, $\bar{s} = \dot{\bar{q}} + \gamma_2 \bar{q}$, $\dot{q}_r = \dot{q}_d - \gamma_2 \tilde{q}$, and $\bar{q} = q - q_d^\star$ $\gamma_2 > 0$ and $\gamma_1 > 0$ are two scalar gains. Let us consider the following positive functions:

$$\begin{array}{rcl} V_1(t,s) & = & \frac{1}{2}s(t)^T M(q)s(t) \\ V_2(t,s) & = & \frac{1}{2}s(t)^T M(q)s(t) + \gamma_2\gamma_1 \tilde{q}(t)^T \tilde{q}(t) \end{array} \tag{9}$$

Control parameters: The control parameters which can be tuned by the end user are feedback gains γ_1, γ_2 and K_f, the gain α and the time $\tau_0^{k_{cyc}}$, which define $q_d^\star$.

3.4 Closed-loop stability analysis

Assumption 1 *The controller U_t in (5) assures that a sequence $\{t_k\}_{k\ge 0}$ of impact times exists, with $\lim_{k\to+\infty} t_k = t_\infty < +\infty$.*

Proposition 1 *Let assumption (1) hold. The system defined by (1) in closed-loop with the controller (5)-(6) and $q_d(\cdot)$, $q_d^\star(\cdot)$ defined as in section 3.2, is:*

(i) - *Asymptotically strongly stable if $q_d^\star(.)$ is designed such that at the first impact time of each phase $I_{k_{cyc}}$ we have*
$$\left[M_{11}(q(t_0))\dot{q}_1(t_0^-) + \dot{q}_2(t_0^-)^T M_{21}(q(t_0)) \right] \dot{q}_{1d}(t_0^-) \le 0.$$

(ii) - *Asymptotically strongly stable if $M_{12} = 0$ and $e_n = 0$.*

(iii) - *Asymptotically weakly stable if $M_{12} = 0$ and $0 \leq e_n < 1$.* ∎

The proof of proposition 1 can be found in [1]. Briefly, the proof shows that the Lyapunov function $V(t)$ in equation (7) decreases on the phase $\Omega_{k_{cyc}}$. And that one has $V(x(t_f^{k_{cyc}}), t_f^{k_{cyc}}) \leq V(x(\tau_0^{k_{cyc}}), \tau_0^{k_{cyc}})$.

Proposition 2 *Let assumption 1 hold, $e_n \in (0,1)$ and $q_{1d}^\star$ be defined as in section 3.2. Consider the system defined by (4) in closed-loop with the controller in (5) and (8).*

(i) - *If the controller $T(q)U$ in (8) assures that $\parallel \tilde{q}(\tau_0^{k_{cyc}}) \parallel < \epsilon$, $\epsilon > 0$ for all k_{cyc} over the cycles, then the system initialized on Ω_0 with $V_2(\tau_0^0) \leq 1$ is therefore pratically Ω-weakly stable with closed-loop state $x(.) = s(.)$.*

(ii) - *If the controller $T(q)U$ in (8) assures that $\parallel \tilde{q}_2(t_{k+1}) \parallel \leq \parallel \tilde{q}_2(t_k) \parallel$, for all t_k on $[t_0, t_\infty)$, then the system initialized on Ω_0 with $V_2(\tau_0^0) \leq 1$ is therefore pratically Ω-weakly stable with closed-loop state $x(.) = [s(.), \tilde{q}(.)]$.* ∎

The proof of proposition 2 can be found in [1]. This proof uses the fact that the control law (8) is exponentially decreasing ($\dot{V}_1(t) \leq -\gamma V_1(t)$ outside phase $I_{k_{cyc}}$).

4   Simulation
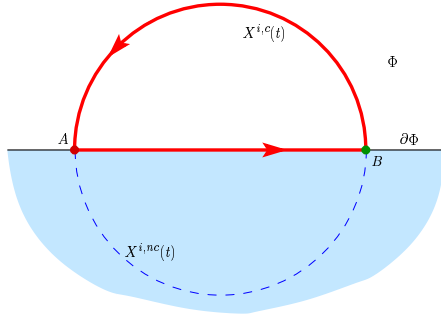
Figure 6:   Half circle reference
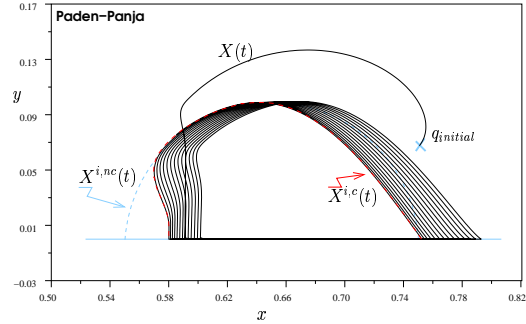
Figure 7: n°3 : Trajectories in the plane Oxy

In this section we show some simulations of the previous control scheme on a planar two-degree of freedom robotic arm (as seen on Fig. 2). The numerical scheme is based on an event driven simulation scheme. The numerical values used for the dynamical model are $l_1 = l_2 = 0.5$m, $I_1 = I_2 = 1$kg.m^2 and $m_1 = m_2 = 1$kg for respectively the length, the inertia
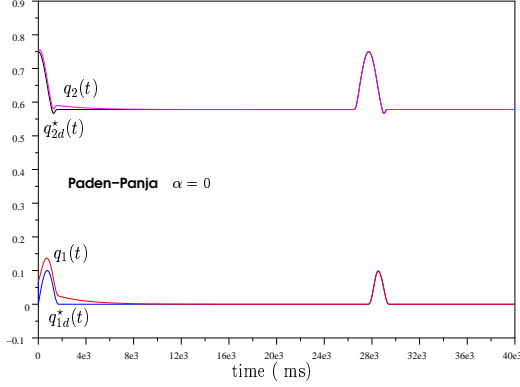
Figure 8: $q_d^\star(t)$ and $q(t)$ for tangential approach
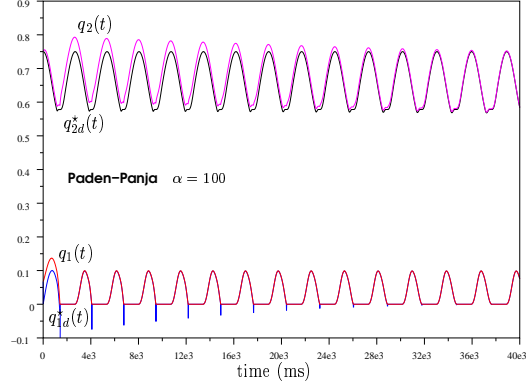
Figure 9: $q_d^\star(t)$ and $q(t)$ for $\alpha = 100$

and the mass of the two links of the arm. The restitution coefficient is set to $e_n = 0.7$. The minimization needed for the computation of the impact law is performed using the FSQP algorithm [4]. In the following examples, the system tracks a circle (see Fig. 6). If nothing else is written on the figures, the gains used for simulations are $\alpha = 100$, $\gamma_1 = 2$, $\gamma_2 = 5$ and $Pe = 3$s for Paden-Panja scheme (Pe is the desired period of one cycle), and $\alpha = 100$, $\gamma_1 = 10$, $\gamma_2 = 0.5$ and $Pe = 4$s for Slotine Li scheme.

On Figs. 8 and 9, we compare our control scheme ($\alpha = 100$) and the tangential approach ($\alpha = 0$). Fig. 8 shows that the tangential approach implies longer stabilisation phases even in the perfect case. This demonstrates the influence of α on the duration of phases $I_{k_{cyc}}$, and consequently on the cycle duration. The Fig. 9 demonstrates the asymptotic convergence of this laws. The desired trajectory $q_{1d}^\star$ goes less and less deeper under the constraint as the cycles go on: the term $-\alpha V(\tau_0^{k_{cyc}})$ decrease as k_{cyc} increase. The evolution of the Lyapunov function $V(t)$ is displayed on Fig. 10. It can be seen that the system converges asymptotically: the first jump of each cycle of the Lyapunov function decreases over the cycles. The hybrid Slotine-Li scheme provided similar results, so they are not presented here. On the zoom of Fig. 10, we see that the Lyapunov function does not fulfil the requirement of the proposition 1: $V(t_k^3) \geq V(\tau_0^3)$. This is logical since $M_{12} \neq 0$. But the system is still stable because the duration of the phase $\Omega_{2k_{cyc}+1}$ is long enough to have $V(t_0^{3-}) \leq V(t_0^{2-})$. On Fig. 7 the orbit of the trajectories can be seen. These orbits converge to a limit cycle. This limit cycle is slightly deformed compared to the desired half circle. This deformation is due to the transition phase $I_{k_{cyc}}$ (when the $q_{2d}^\star$ trajectories are frozen) and due to the take off phase (when $q_{1d}^\star$ and $q_{2d}^\star$ signals need to be resynchronized since the take-off time is not known precisely). Finally from the point of view of the end-user, the real tracking error is $X^{i,nc} - X$ (X tends to $X^{i,c}$ asymptotically over cycles). The end user can reduce this error by decreasing the speed used to performed a cycle (as seen on
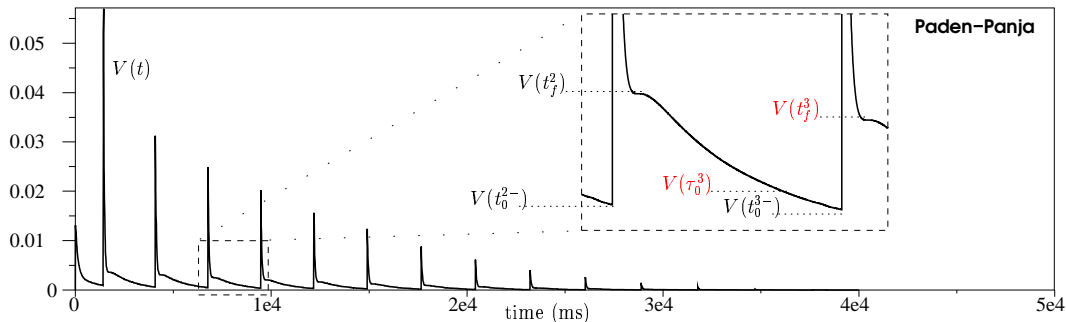
Figure 10: Evolution of the Lyapunov function

Fig. 18 where the cycle period is set to 16s against 3s for the previous test). Each control law (U_{nc},U_c,U_t) considered separately possesses good robustness properties (because U_{nc} and U_c are passivity-based, and U_t creates a bouncing-ball dynamics). The problem is: Is this robustness conserved when switching between these 3 controllers as described in sec. 3 ?

5   Dynamical parameters uncertainties

This section deals with the robustness of this control scheme with respect to uncertainties in the parameters of the control laws (6) and (8). The dynamical model used in the dynamic integration part of the simulator is the same as in the previous section. The model used in the computation of the input torque $T(q)U$ uses mass 30% heavier ($m_1 = m_2 = 1.3$kg). Figs. 11-12 show results for the hybrid Paden-Panja scheme, and Figs. 13-14 show the hybrid Slotine-Li one. These two tests point out that uncertainty in the dynamic model caused tracking error to increase when the reference trajectories vary quickly (as seen on zooms of the Figs. 11-13).

Small variations of the tracking error imply small variations of the Lyapunov function (Figs. 12 and 14), then the system is no more asymptotically stable. Even if the function $V(t)$ become very small, there are always small impacts. Then some small discontinuities can be seen, at each first impact, on Figs. 12 and 14 ($\sigma_V(t_0)$ is positive).

In conclusion, we can say that this control scheme is robust with respect to the uncertainty on the dynamic model, but errors on the model imply that asymptotic convergence is lost. Secondly, the hybrid Slotine Li scheme is more robust that the hybrid Paden-Panja: on these simulations, the Lyapunov's function peaks are about $3e^{-4}$ for Slotine Li law against $5e^{-3}$ for Paden Panja scheme.
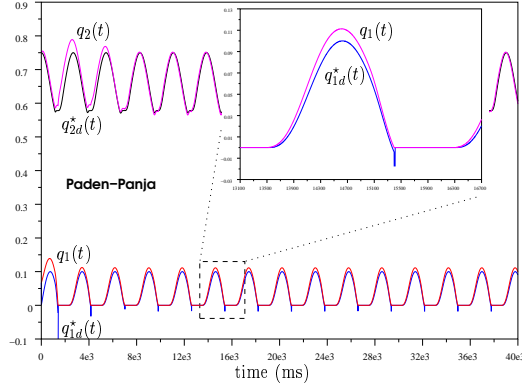
Figure 11: Robustness - $q_d(t)$ and $q(t)$
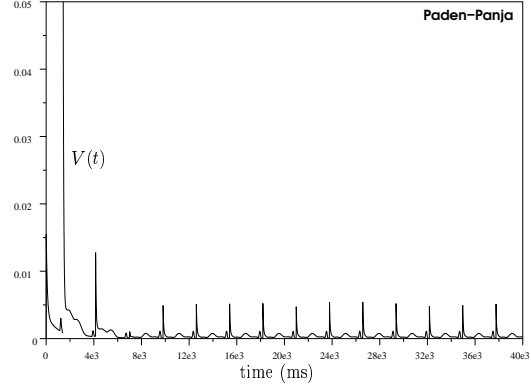
Figure 12: Robustness - function $V(t)$
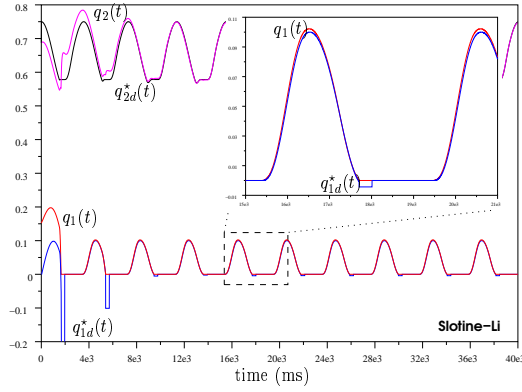
Figure 13: Robustness - $q_d(t)$ and $q(t)$
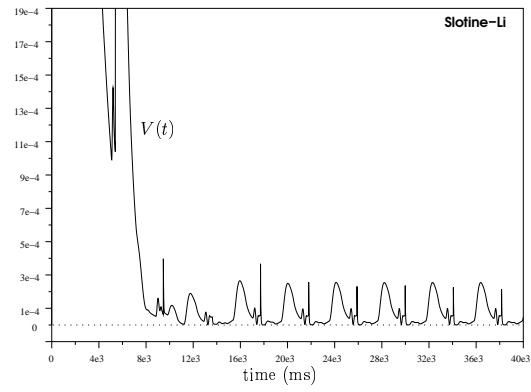
Figure 14: Robustness - function $V(t)$

6 Constraint position uncertainty

In this section, we study the robustness of the controller with respect to the uncertainty on the constraint position. The location of the constraint surface is not known accurately. Two situations may be considered.

1- The estimated position (denoted by $\hat{q}_{1c}$) of the constraint is lower than the real position (denoted by q_{1c}), i.e. $\hat{q}_{1c} = q_{1c} + c$ with $c < 0$ (c denotes the error of estimation).

2- The estimated position of the constraint is above the real position. i.e. $c > 0$.

Case 1 $c < 0$: In this case the desired trajectories decrease toward $q_{1d}(\tau_1^{k_{cyc}}) = -\alpha V(\tau_0^{k_{cyc}}) - |c|$ instead of $q_{1d}(\tau_1^{k_{cyc}}) = -\alpha V(\tau_0^{k_{cyc}})$. The error c can be incorporated
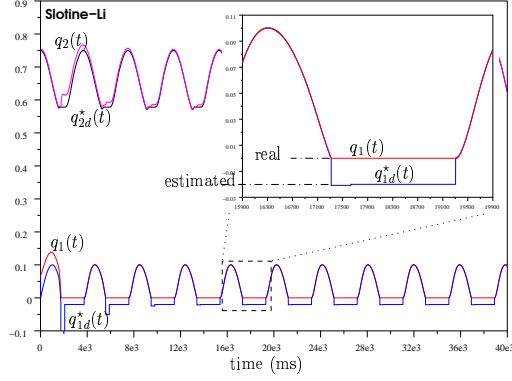
Figure 15: Under estimated constraint
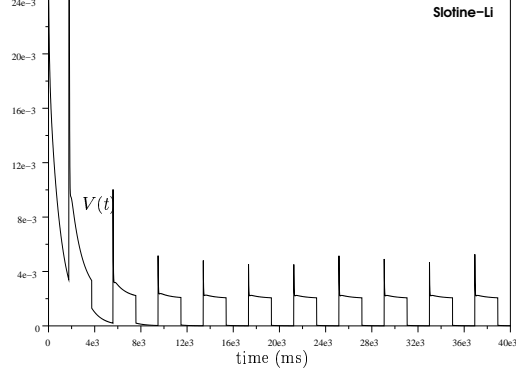
Figure 16: Error on $V(t)$

in the term $-\alpha V(\tau_0^{k_{cyc}})$ and the stability of the transition phase is not changed. During the constraint phase the controller is:

$$U_c = U_{nc} - (P_d + \gamma_1[|c|\ 0]^T) + K_f(P_q - P_d) \tag{10}$$

The error term $\gamma_1|c|$ is added to the desired force P_d and contributes to keep the contact with the surface during the constrained phase.

The system remains stable but it loses its asymptotic stability: If the tracking is perfect $V(\tau_0^{k_{cyc}}) = 0$ and $q_{1d}^\star = -|c|$, so that the system does not approach the surface tangentially and rebounds occur. An example is depicted on Figs. 15-16.

Case 2 $c > 0$: If the tracking is perfect $V(\tau_0^{k_{cyc}}) = 0$, the desired trajectory decreases toward $q_{1d} = c$ and the system never reaches the constraint. There is no convergence (see Fig. 17 after two cycles). This problem can be solved by monitoring the time of stabilization. If there is no stabilization after an estimated time $\hat{t}_\infty$, the estimated position of the constraint is refreshed as $\hat{q}_{1c}^{new} = \hat{q}_{1c}^{old} - \epsilon$. After a finite number of iterations, one gets $\hat{q}_{1c} < 0$. The system is in the previous situation $c < 0$ and the stability is preserved. Figs. 19-20 shows an example of self-adjustment of the estimated position of the constraint. At the beginning of the simulation $\hat{q}_{1c}$ was set to 2cm. The increment of correction ϵ is set to 1.5cm. Then, at the end of the simulation, one has $\hat{q}_{1c} = 2 - 2 \times 1.5 = -1$cm. The error of estimation become negative $c = -1$cm.

When tracking is not perfect and $\alpha V(\tau_0^{k_{cyc}}) > c$ (like during the first two cycles of simulations on Figs. 17 and 19), the transition phase is able to stabilize the system on the surface $\partial\Phi$. But during the constraint phase, the controller is:

$$U_c = U_{nc} - (P_d - \gamma_1[c\ 0]) + K_f(P_q - P_d) \tag{11}$$

P_d must be chosen large enough compared to $\gamma_1 c$ to be sure that the system keeps the contact with the surface during the whole constraint phase.
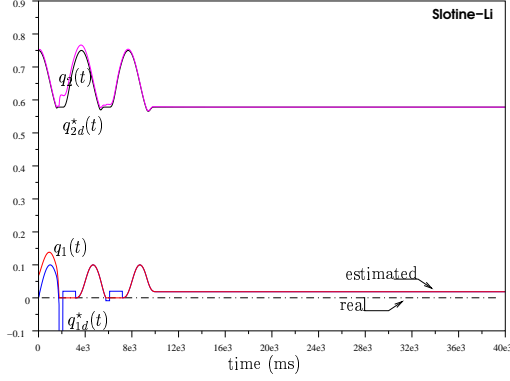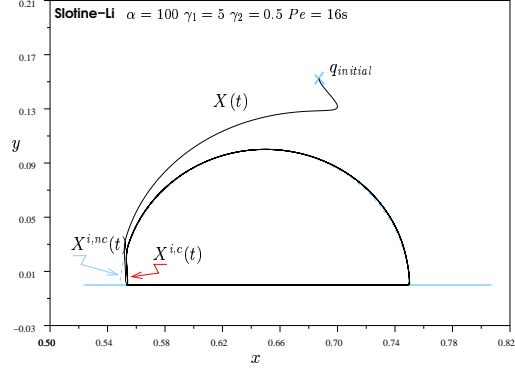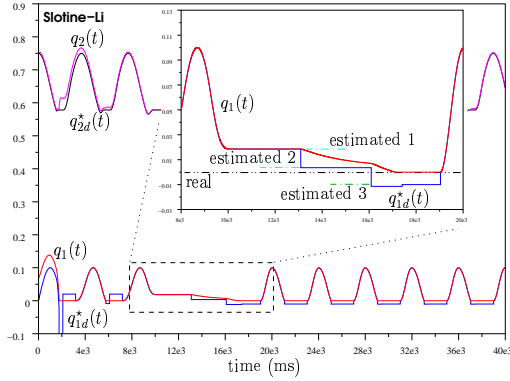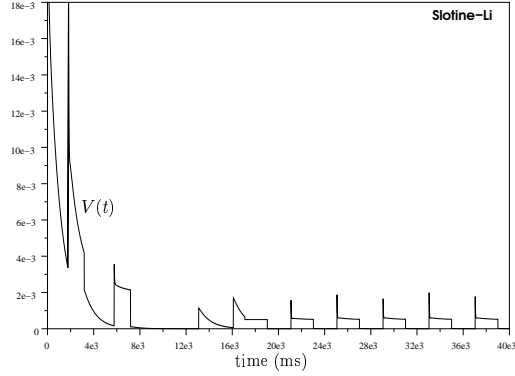
Figure 17: No detection of the impact

Figure 18: Orbits in the plane Oxy

Figure 19: On-line estimation of c

Figure 20: Error on $V(t)$

In conclusion we can say that this control scheme is robust with respect to uncertainty on the constraint position if the estimated position is lower than the real (case 1 with $c \leq 0$). In the second case, the controller scheme is robust only if we add to the supervisor a high-level decision law which monitor if contact occur or not. Then decide if this non-attendance of contact is due to constraint position error or due to anything else.

7 Robustness with respect to the measurement noise

This section deals with the robustness of this control scheme with respect to measurement noise on position and velocity. Figs. 21-22 show the Lyapunov function of the two control schemes, respectively the Paden-Panja scheme with white noise of 5% added on q and $\dot{q}$,
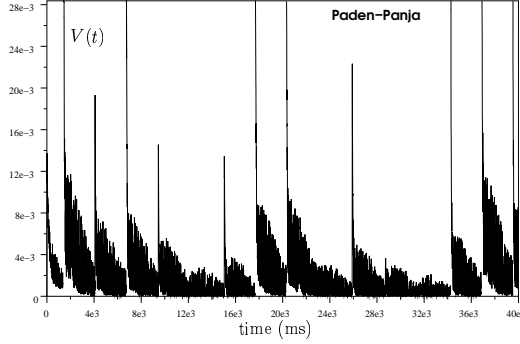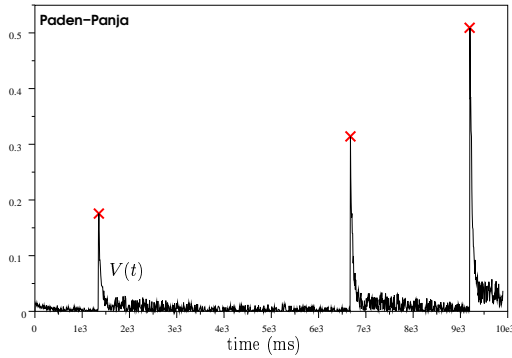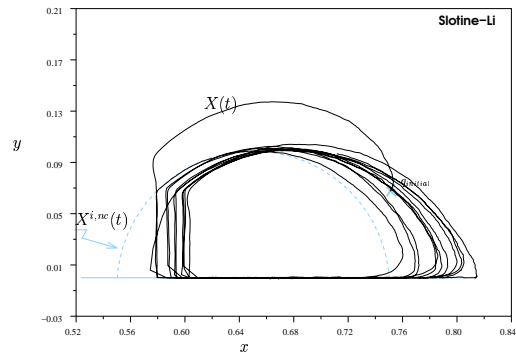
Figure 21: Robustness -function $V(t)$
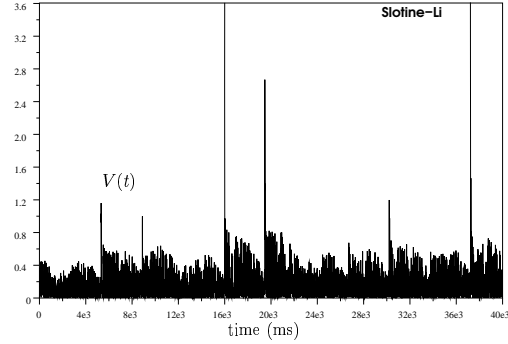
Figure 22: Robustness - function $V(t)$

Figure 23: Robustness - function $V(t)$

Figure 24: Robustness - trajectories

and the Slotine-Li law with noise level of 40%. These noise levels are the maximum for each law before instability.

Fig. 23 shows the evolution of the Lyapunov function of a simulation of the Paden-Panja scheme at the limit of the stability, with a noise level of 10%. The jumps $\sigma_V(\tau_0^{k_{cyc}})$ increase over the cycles. This example is not robust because it doesn't fulfil all requirements of proposition 1 (see remark on Fig. 10 sec. 4).

From these simulations, we conclude that the hybrid Slotine-Li scheme is more robust than the hybrid Paden-Panja one. But on Fig. 24, we see than even if the closed loop system does not diverge when the noise level is set to 40%, then the tracking control is very bad with such noise. Exponential stability improves robustness of the hybrid Slotine-Li controller.

Another important point to deal with is the magnitude of the force control. If the force controller gains (k_f) and reference (P_d) are too small, then the noise on the measurement of the position can induce unwanted detachment during the permanently constraint phase.

8 Conclusions

The aim of this paper is to study the robustness of nonsmooth passivity based controllers with respect to errors on the dynamical model parameters, to the constraint position knowledge and to the measurement noise. We study the extension of two laws to the case of nonsmooth dynamic: the Paden Panja PD+ controller the Slotine Li control law. These two laws are robust with respect to dynamical model errors. They are very robust if the constraint position is under-estimated. In the case of constraint estimated above the real position, we present a solution to resolve this difficulty. Finally the hybrid Slotine-Li controller is very robust with respect to measurement noise whereas the hybrid Paden-Panja scheme is much less robust.

Globally the hybrid Slotine-Li scheme is more robust than the hybrid Paden Panja scheme: as explained above, this is due to the fact that stability conditions are easier to fulfil for Slotine-Li (proposition 2) than for Paden-Panja scheme (proposition 1). These results are validated on numerical simulations.

References

[1] Bourgeot, J.M., Brogliato, B. : Tracking control of complementarity Lagrangian systems. The International Journal of Bifurcation and Chaos, special issue on Nonsmooth Dynamical Systems (associed editor J. Awrejwicz). **15**(3) (2005) (to appear)

[2] Brogliato, B., Niculescu, S., Orhant, P. : On the control of finite dimensional mechanical systems with unilateral constraints. IEEE Trans. on Automatic Control. **42**(2) (1997) 200–215

[3] Brogliato, B., Niculescu, S., Monteiro-Marques, M. : On tracking control of a class of complementary-slackness mechanical systems. Systems and Control Letters. **39**(4) (2000) 255–266

[4] Lawrence, C.T., Zhou, J.L., Tits., A.L.: `http://www.isr.umd.edu/labs/cacse/fsqp/fsqp_dist.html`. (1998)

[5] McClamroch, N., Wang, D. : Feedback stabilization and tracking of constrained robots. IEEE Trans. on Automatic Control **33**(5) (1988) 419–426

[6] Moreau, J.J. : Unilateral contact and dry friction in finite freedom dynamics. Nonsmooth Mechanics and Applications, CISM Courses and Lectures no 302 Springer-Verlag (1988)

[7] Paden, B., Panja, R. : Globally asymptotically stable PD+ controller for robot manipulators. Int. J. Control. **47**(6) (1988) 1697–1712

[8] Slotine, J.J., Li, W. : Adaptive manipulator control: a case study. IEEE Trans. on Automatic Control. **33**(11) (1988) 995–1003

Contents